Exciton Storage by Mn 2+ in Colloidal Mn 2+ – Doped CdSe Quantum Dots

5 AUTHORS, INCLUDING:

Jos van Rijssel
Utrecht University
14 PUBLICATIONS **246** CITATIONS

SEE PROFILE

Andries Meijerink
Utrecht University
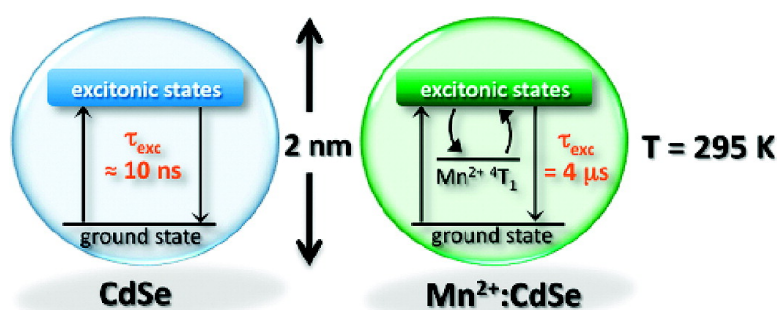**364** PUBLICATIONS **13,512** CITATIONS

SEE PROFILE

Letter

Exciton Storage by Mn in Colloidal Mn-Doped CdSe Quantum Dots

Re#mi Beaulac, Paul I. Archer, Jos van Rijssel, Andries Meijerink, and Daniel R. Gamelin

More About This Article

Additional resources and features associated with this article are available within the HTML version:

- Supporting Information
- Links to the 2 articles that cite this article, as of the time of this article download
- Access to high resolution figures
- Links to articles and content related to this article
- Copyright permission to reproduce figures and/or text from this article

View the Full Text HTML

Exciton Storage by Mn^{2+} in Colloidal Mn^{2+}-Doped CdSe Quantum Dots

Rémi Beaulac,[†] Paul I. Archer,[†] Jos van Rijssel,[‡] Andries Meijerink,[‡] and Daniel R. Gamelin*,[†]

Department of Chemistry, University of Washington, Seattle, Washington 98195-1700, and Department of Condensed Matter, Debye Institute, Utrecht University, Princetonplein 5, P.O. Box 80 000, 3508 TA Utrecht, The Netherlands

ABSTRACT

Colloidal Mn^{2+}-doped CdSe quantum dots showing long excitonic photoluminescence decay times of up to $\tau_{exc} = 15\ \mu$s at temperatures over 100 K are described. These decay times exceed those of undoped CdSe quantum dots by $\sim 10^3$ and are shown to arise from the creation of excitons by back energy transfer from excited Mn^{2+} dopant ions. A kinetic model describing thermal equilibrium between Mn^{2+} $^4T_1$ and CdSe excitonic excited states reproduces the experimental observations and reveals that, for some quantum dots, excitons can emit with near unity probability despite being ~ 100 meV above the Mn^{2+} $^4T_1$ state. The effect of Mn^{2+} doping on CdSe quantum dot luminescence at high temperatures is thus completely opposite from that at low temperatures described previously.

For over a decade, researchers have been scrutinizing the photophysical properties of Mn^{2+}-doped CdSe nanostructures.[1,2] In the physics community, self-assembled Mn^{2+}-doped CdSe quantum dots (Mn^{2+}:CdSe QDs) have been prepared by molecular beam epitaxy (MBE) or related techniques and examined by photoluminescence (PL) and magneto-PL spectroscopies in order to understand carrier spin dynamics and carrier−dopant magnetic exchange interactions in spatially confined systems.[1−9] In the chemistry community, the synthetic challenge of incorporating Mn^{2+} impurity ions within colloidal CdSe QDs[10] has hindered investigation of similar photophysical phenomena in freestanding nanocrystals; but this challenge can now be overcome, and magneto-absorption and magneto-PL experiments have recently demonstrated "giant" excitonic Zeeman splittings in colloidal Mn^{2+}-doped CdSe QDs that are comparable in magnitude to those of their best MBE-grown cousins.[11,12] In these colloidal Mn^{2+}:CdSe QDs, quantum confinement allows continuous tuning of the first excitonic excited-state from below all Mn^{2+} excited states (bulk limit) to above the lowest Mn^{2+} excited state ($^4T_1$), simply by reducing the spherical QD diameter.[12] Whereas the PL of large Mn^{2+}:CdSe QDs is dominated by excitonic recombination, the PL of the small QDs is dominated by sensitized Mn^{2+} emission. In the latter size regime, rapid energy transfer to Mn^{2+} has been reported to reduce the excitonic PL decay time from nano- or microseconds down to picoseconds in studies of MBE-grown Mn^{2+}:CdSe QDs and related materials.[2,13]

In this Communication, we show that the above description of nanosecond excitonic PL decay times for large Mn^{2+}:CdSe QDs and picosecond excitonic PL decay times for small QDs only applies to the two extremes of the quantum confinement spectrum, and only at low temperatures. By using colloidal Mn^{2+}-doped CdSe QDs, it is demonstrated that in intermediate cases the observed CdSe QD excitonic PL decay times (τ_{exc}) can be dramatically *increased* at elevated temperatures by Mn^{2+} doping, to as long as 15 μs at temperatures above 100 K. This phenomenon is not due to perturbation of the CdSe QD electronic structure per se, but reflects storage of the photoexcitation energy in an embedded long-lived Mn^{2+} excited-state reservoir prior to its thermally activated release via excitonic PL.

Colloidal Mn^{2+}-doped CdSe QDs of different average diameters (d) were prepared and characterized as described in detail previously.[11,12,14] PL data were also collected as described previously.[15] The lower spectrum of Figure 1 plots the 5 K PL of $d \approx 2.2$ nm, $0.4 \pm 0.2\%$ Mn^{2+}:CdSe QDs collected using continuous wave (CW) excitation. Two PL features are observed: the band at 2.44 eV is the CdSe excitonic PL, and the band at 2.12 eV is the Mn^{2+} $^4T_1 \rightarrow\ ^6A_1$ ligand-field transition.[12] The inset shows a collection of data adapted from ref 12 describing the dependence of these two PL energies on CdSe QD diameter. Whereas the energy of the Mn^{2+} ligand-field transition is independent of nanocrystal diameter, the excitonic PL energy shifts because of quantum confinement, and the nature of the lowest energy emission changes when the two cross at $d \approx 3.3$ nm.

Figure 1 also includes the 5 K PL spectrum of the same sample collected under quasi-gated conditions. This experi-
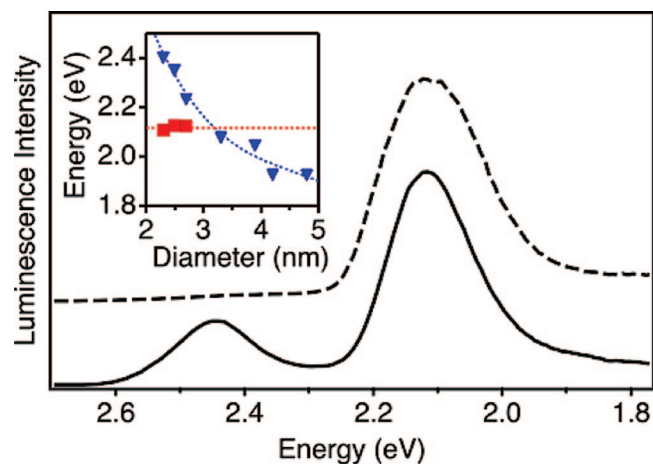

Figure 1. 5 K PL spectra of colloidal $d \approx 2.2$ nm, $0.4 \pm 0.2\%$ Mn^{2+}-doped CdSe QDs collected under continuous (solid) and gated (dashed) conditions ($E_{excitation} = 2.79$ eV for both). Inset: Data from ref 12 showing dependence of excitonic (triangles) and Mn^{2+} $^4T_1$ (squares) PL maxima on d.

Figure 2. 5 K (blue) and 200 K (red) PL decay curves plotted on a linear intensity scale: (a) Mn^{2+} $^4T_1 \rightarrow {}^6A_1$ PL for $d \approx 2.2$ nm, $0.4 \pm 0.2\%$ Mn^{2+}:CdSe QDs. (b) Excitonic PL for $d \approx 2.2$ nm, $0.4 \pm 0.2\%$ Mn^{2+}:CdSe QDs. Note the $\sim10^4$ increase in time scale at 200 K. (c) Excitonic PL for $d \approx 4.3$ nm, $4.5 \pm 0.2\%$ Mn^{2+}:CdSe QDs. ($E_{excitation} = 2.79$ eV)

ment allows discrimination against quickly decaying PL intensities following nanosecond pulsed excitation at a 10 Hz repetition rate (Lambda Physik LPD dye laser, Coumarine 120 dye, pumped by an LPX100 Excimer laser) by suppressing signals within the ~10 ns saturation recovery time of the detector (Hamamatsu R928). This spectrum thus reports intensities integrated over all times greater than $t \sim 10$ ns following the excitation pulse. As seen from comparison with the CW spectrum, the 5 K excitonic PL is effectively eliminated in the gated spectrum, indicating that the observed excitonic PL decay time is short ($\tau_{exc} \leq \sim10$ ns), but the relative Mn^{2+} PL intensity is strongly enhanced, indicating the Mn^{2+} PL decay time (τ_{Mn}) greatly exceeds 10 ns.

More precise decay times were obtained by monitoring the PL decay kinetics following pulsed dye laser excitation, from which the Mn^{2+} PL was found to decay with $\tau_{Mn} = 273$ μs at 5 K (Figure 2a). Decay times for the fast excitonic emission were measured using a blue (441 nm) picosecond diode laser for excitation and a fast PMT (Hamamatsu H7421−50) in combination with time correlated photon counting for detection. Two excitonic PL decay timescales were observed: $\tau_{exc,1} < 1$ ns ($\sim20\%$) and $\tau_{exc,2} = 43$ ns ($\sim80\%$; Figure 2b inset). The fast component of the excitonic PL decay agrees well with the subnanosecond exciton−Mn^{2+} energy transfer timescales reported for related MBE-grown Mn^{2+}:CdSe QDs (e.g., $15-100^{2,13}$ ps). The slower component derives from the subset of QDs containing no Mn^{2+} ions and is similar in magnitude to the 5 K PL decay times measured for undoped CdSe QDs of comparable diameter.[15] At this low dopant concentration, the average number of Mn^{2+} ions per nanocrystal is ~0.4. Most QDs thus contain either 0 (67%) or 1 (28%) Mn^{2+} ion.

For the purposes of comparison, Figure 2c shows the 5 K excitonic PL decay curve measured for large Mn^{2+}:CdSe QDs ($d \approx 4.3$ nm, $4.5 \pm 0.2\%$ Mn^{2+}), where the Mn^{2+} excited states are outside of the bandgap and consequently only excitonic PL is observed (cf. Figure 1 inset). This
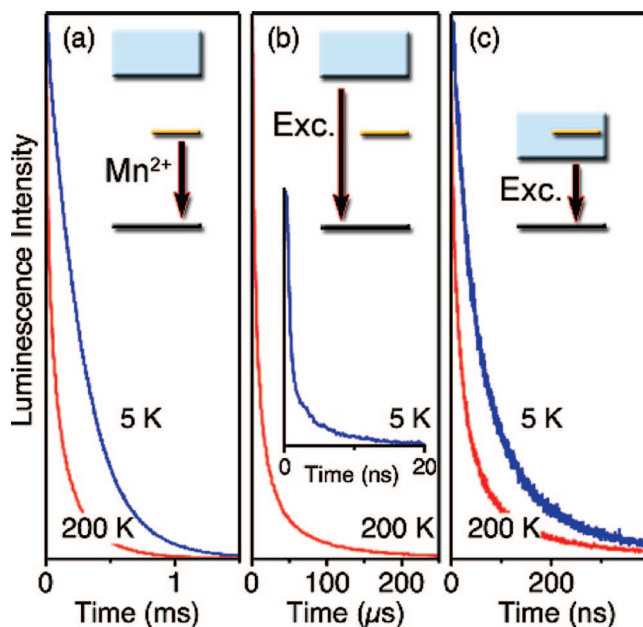
excitonic PL decay is multiexponential, suggesting a distribution in the rates of nonradiative processes,[16,17] but it can be fitted with two major components: $\tau_{exc,1} = 39$ ns ($\sim35\%$) and $\tau_{exc,2} = 136$ ns ($\sim65\%$), in reasonable agreement with 5 K PL decay times measured for undoped CdSe QDs of comparable diameter.[15] The comparison of Figure 2b,c shows that shifting the exciton to above the Mn^{2+} $^4T_1$ excited state quenches the 5 K excitonic PL via rapid energy transfer to Mn^{2+}, whereas shifting the exciton to below the Mn^{2+} $^4T_1$ excited state leads to excitonic emission with excitonic PL decay times similar to those of the undoped analogues, even in cases of relatively high Mn^{2+} concentrations such as the sample shown in Figure 2c. Overall, these results thus agree well with those found for MBE-grown Mn^{2+}:CdSe QDs,[2,13] indicating that the colloidal QDs under consideration here are also representative of those grown by MBE.

Interesting effects are observed as the temperature of the sample from Figure 1 is raised. Figure 3a,b shows CW and gated PL spectra obtained at various temperatures between 25 and 185 K. In both experiments, the Mn^{2+} PL intensity decreases smoothly with increasing temperature. In the CW spectra, the excitonic PL intensity decreases and then increases again with increasing temperature, while shifting continuously to lower energy. In the gated PL spectra, excitonic PL intensity is extremely weak at 5 K (Figure 1) but grows in above ~75 K and shifts to higher energy with increasing temperature, starting from much lower energies than the excitonic band in the CW emission spectrum (Figure 3b). For both measurements, the excitonic PL temperature dependence is completely different from the well-known Varshni-like red shift observed in parallel measurements on undoped CdSe QDs (data not shown). This unusual spectral
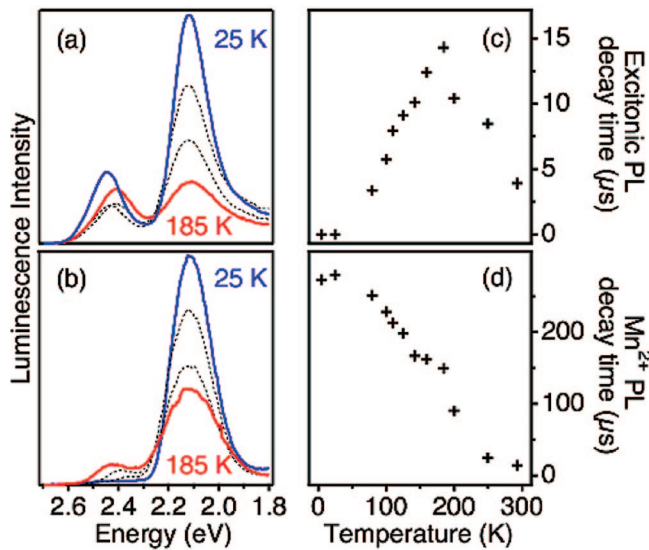
Figure 3. Variable-temperature CW (a) and gated (b) PL data for colloidal $d \approx 2.2$ nm, $0.4 \pm 0.2\%$ Mn^{2+}-doped CdSe QDs (25, 100, 142, 185 K). (c) Average excitonic PL decay times, measured at 2.36 eV. (d) Average Mn^{2+} PL decay times, measured at 2.12 eV. ($E_{\text{excitation}} = 2.79$ eV)

temperature dependence is accompanied by an equally unusual temperature dependence of τ_{exc}. Figure 2b shows that as the temperature is raised from 5 to 200 K, τ_{exc} of the small Mn^{2+}:CdSe QDs increases tremendously, in contrast with the behavior of undoped CdSe QDs[15,18] or of the large Mn^{2+}:CdSe QDs (Figure 2c). The decays are clearly multi-exponential but are described well by double-exponential functions, from which intensity-average τ_{exc} values have been obtained. Figure 3c plots these average τ_{exc} values versus temperature between 5 and 300 K. Whereas $\tau_{\text{exc}} < 1$ ns at 5 K, the same excitonic intensity decays with $\tau_{\text{exc}} = 14$ μs at 185 K. The excitonic PL decay thus lengthens by $>10^4$ upon sample warming. Over the same temperature range, the average value of τ_{Mn}, which is also multiexponential, decreases only moderately from 273 to 149 μs (Figure 3d). An inverse relationship between τ_{exc} and τ_{Mn} is clearly observed in the 5−185 K temperature range (Figure 3c,d). Other nonradiative processes (e.g., thermally activated energy migration to surface traps) likely contribute to the decreasing PL intensities and decay times above 200 K. At room temperature, $\tau_{\text{exc}} = 4$ μs and is obviously lengthened by the presence of the Mn^{2+} dopants, even though Mn^{2+} PL is nearly absent.

We propose that the unusual excitonic PL temperature dependence (Figure 3a,b) and the extremely long excitonic PL decay times (Figure 2b and Figure 3c) of these small Mn^{2+}:CdSe QDs reflect thermal population dynamics involving the long-lived $^4T_1$ state of the Mn^{2+} dopants and the QD excitonic states, separated by an energy gap ΔE (Figure 4a). To test this hypothesis, the gated excitonic PL spectra of Figure 3b were modeled using eq 1a, which describes this scenario. The relevant energy gap is that between the Mn^{2+} $^4T_1$ electronic origin ($E_{00}(^4T_1)$ in the PL spectrum) and the emissive excitonic level. From the Poissonian Mn^{2+} PL band shape in Figure 1, $E_{00}(^4T_1) = 2.263$ eV in Mn^{2+}:CdSe.

Because of the finite particle size distribution, a distribution of exciton energies exists within the same ensemble sample. For these measurements, this distribution is very useful because it generates a continuous distribution in ΔE that allows spectral intensity distributions to be related to thermal free energies. The energy gap distribution function used for the simulation was taken as the difference between $E_{00}(^4T_1)$ and the experimental CW excitonic PL band shape ($f_{\text{exc}}(E)$) at each temperature, yielding ΔE values ranging from 0 to $\sim$370 meV. The probability of excitonic emission (P_{exc}) for any specific ΔE and T is then determined by the thermal population of that exciton and the intrinsic rate constants for the exciton and Mn^{2+} decays (k_{exc} and k_{Mn}, respectively).

$$I_{exc}(E,T) = f_{exc}(E,T) \times P_{exc}(\Delta E, T) \quad \text{(1a)}$$

$$P_{exc}(\Delta E, T) = \frac{k_{exc}\exp(^{-\Delta E}/_{kT})}{k_{Mn}\exp(^{-\Delta E}/_{kT}) + k_{exc}(1 - \exp(^{-\Delta E}/_{kT}))} \quad \text{(1b)}$$

In the limit where the rate constants for energy transfer between the two excited states are much greater than both k_{exc} and k_{Mn}, $P_{\text{exc}}(\Delta E,T)$ is given by eq 1b. Note that k_{exc} and k_{Mn} are the intrinsic decay rate constants (i.e., that would describe the decay kinetics of each state in the absence of the other), whereas the measured PL decay times shown in Figure 2 (τ_{exc} and τ_{Mn}) are those of the coupled system in which these two states coexist. k_{exc} is known from the literature[15,18] to be $\sim$10[8] s^{-1}, and k_{Mn} was taken from the 5 K Mn^{2+} PL decay time (Figure 2a), where thermal back energy transfer does not occur. By using $k_{\text{exc}} = 10^8$ s^{-1}, $k_{\text{Mn}} = 3.7 \times 10^3$ s^{-1}, and the temperature dependence of both $f_{\text{exc}}(E)$ and ΔE from the experimental CW PL spectra, eq 1b thus allows simulation of the variable-temperature gated excitonic PL spectra from Figure 3 with no adjustable parameters. For simplicity, both k_{exc} and k_{Mn} were assumed to be temperature independent.

The results of this simulation for temperatures between 100 and 200 K are presented in Figure 4b, where they are compared with the experimental data in the same energy and temperature range on an expanded scale. From this comparison, it can be seen that this simple model provides an excellent reproduction of the two major experimental observations, namely, the increasing excitonic intensity and the blue-shifting excitonic PL maximum with increasing temperature. A better quantitative reproduction could undoubtedly be achieved by accounting for the temperature dependence of k_{exc} and k_{Mn}, size-dependent excitonic PL intensities, level multiplicities, or the intensity dependence of the quasi-gated detection, but expansion of the model to include such additional variables would not alter or improve our understanding of the main physical effect that is observed. We therefore conclude that the model described by eq 1 correctly captures the essence of the experimental observations. Within this model, analysis of P_{exc} itself reveals that at each temperature the probability of excitonic PL ranges from $\sim$1.0 for QDs with small ΔE to $\sim$0.0 for QDs with large ΔE within the experimental size distribution (Figure 4c). As the temperature increases, P_{exc} increases for QDs with larger ΔE, and the PL maximum blue-shifts accordingly. For some QDs, the probability that an emitted photon detected on the 10 μs
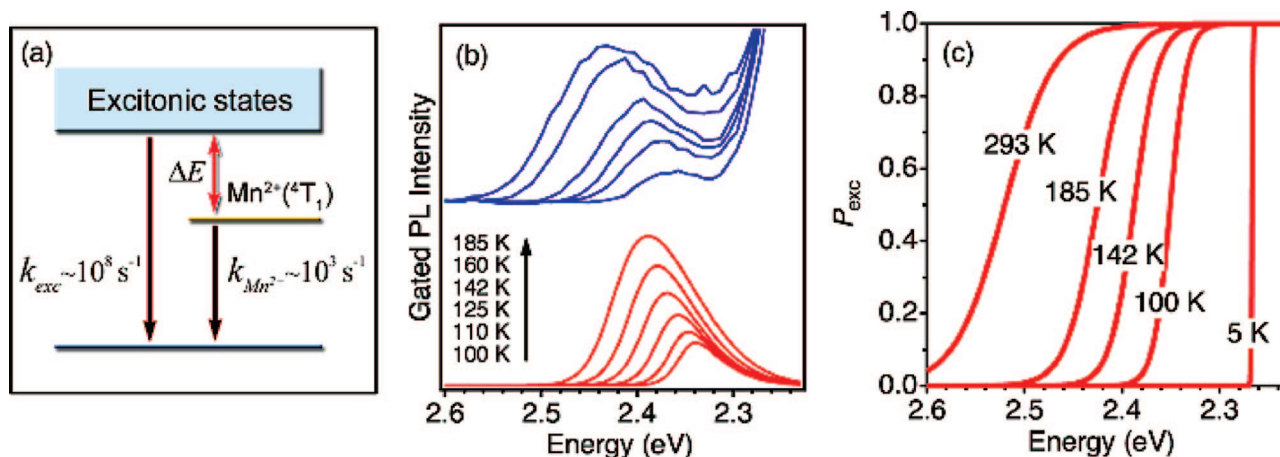
Figure 4. (a) Schematic illustration of the equilibrium model used. (b) Calculated and experimental excitonic PL spectra vs temperature between 100 and 185 K. (c) Probability of excitonic emission (P_{exc}) as a function of its energy for various temperatures. The Mn^{2+} electronic origin occurs at $E_{00}(^4T_1) = 2.263$ eV.

time scale comes from the exciton is thus near unity, despite the fact that the exciton lies >100 meV above the Mn^{2+} $^4T_1$ state and the exciton–Mn^{2+} energy transfer occurs on the subnanosecond time scale. At elevated temperatures, therefore, Mn^{2+} doping does not quench the excitonic PL of small Mn^{2+}:CdSe QDs, but instead, the Mn^{2+} PL is itself quenched by thermally assisted back energy transfer to the excitonic states. This remarkable situation arises because k_{exc} and k_{Mn} differ by $\sim 10^5$.

The observation of excitonic PL decay on timescales 10^3 times longer than the intrinsic excitonic PL lifetime is indicative of exciton storage. Previously, exciton storage involving charge separation across interfaces has been demonstrated.[19−21] The present case is fundamentally different from these previous examples because it involves energy trapping rather than charge trapping. A closer analogy can be drawn between the thermal back energy transfer observed here and that occurring between "dark" and "bright" excitons of undoped colloidal CdSe QDs. In the latter, the longest exitonic PL decay times are $\tau_{exc} \sim 1.25$ μs at $T <$ ~ 2.5 K, with τ_{exc} only ~ 15 ns at 185 K.[15,18] The gradual lengthening of τ_{exc} below ~ 100 K could be reproduced using a thermal equilibrium model similar to eq 1a, with dark–bright energy gaps of only $\sim 0.5 - 2.0$ meV and dark exciton lifetimes of only $0.3-1.4$ μs, both size dependent.[15] Because the dark–bright energy gaps are relatively small, the action of the dark state as a reservoir feeding the bright state is not as clear as in the present Mn^{2+}:CdSe QDs, where the reservoir is the $^4T_1$ excited state of Mn^{2+} and the relevant energy gap can be tuned over a much broader range by changing the CdSe QD diameter (Figure 1 inset). Additionally, whereas the dark-exciton lifetime is sensitive to nanocrystal shape anisotropy and size, the radiative lifetime of Mn^{2+} in CdSe (~ 273 μs, Figure 2b) is determined primarily by spin–orbit coupling, and secondarily by Mn^{2+}–Mn^{2+} exchange interactions (negligible at the present Mn^{2+} concentrations), and it is therefore independent of nanocrystal shape and size. The Mn^{2+} $^4T_1$ excited state is substantially "darker" than the "dark" exciton, and it can therefore extend the excitonic PL decay time much longer

for Mn^{2+}:CdSe QDs than the dark–bright excitonic equilibrium can for undoped CdSe QDs. Finally, the $\sim 10^5$-fold difference between k_{exc} and k_{Mn} allows excitonic emission to occur with near unity probability at elevated temperatures despite having Mn^{2+} states within the gap.

In summary, long excitonic PL decay times have been observed in colloidal Mn^{2+}:CdSe QDs at elevated temperatures and have been shown to arise from thermal equilibrium between the CdSe excitonic states and the very long-lived $^4T_1$ ligand-field excited state of the Mn^{2+} dopants. This result provides an exception to the otherwise general rule that excitonic PL is quenched on the subnanosecond time scale when dopant excited states fall within the semiconductor optical gap. It demonstrates that this rule applies only when the energy gap greatly exceeds kT such that thermal back energy transfer cannot occur within the lifetime of the dopant excited state. For cases in which the Mn^{2+} $^4T_1$ state exists within the gap but has excitonic states within thermal reach, doping can have precisely the opposite effect and lengthen the excitonic PL decay time by several orders of magnitude. The existence of such long excitonic PL decay times in DMS nanocrystals at high temperatures could have interesting ramifications in photonics or spin-photonics technologies.

References

(1) Bacher, G.; Schömig, H.; Scheibner, M.; Forchel, A.; Maksimov, A. A.; Chernenko, A. V.; Dorozhkin, P. S.; Kulakovskii, V. D.; Kennedy, T.; Reinecke, T. L. *Physica E* **2005**, *26*, 37–44.

(2) Oka, Y.; Kayanuma, K.; Shirotori, S.; Murayama, A.; Souma, I.; Chen, Z. *J. Lumin.* **2002**, *100*, 175–190.

(3) Oka, Y.; Shen, J.; Takabayashi, K.; Takahashi, N.; Mitsu, H.; Souma, I.; Pittini, R. *J. Lumin.* **1999**, *83−84*, 83–89.

(4) Kratzert, P. R.; Puls, J.; Rabe, M.; Henneberger, F. *Appl. Phys. Lett.* **2001**, *79*, 2814–2816.

(5) Mackowski, S.; Lee, S.; Furdyna, J. K.; Dobrowolska, M.; Prechtl, G.; Heiss, W.; Kossut, J.; Karczewski, G. *Phys. Stat. Sol. (B)* **2002**, *229*, 469–472.

(6) Hundt, A.; Puls, J.; Henneberger, F. *Phys. Rev. B* **2004**, *69*, 121309(R)

(7) Chernenko, A. V.; Dorozhkin, P. S.; Kulakovskii, V. D.; Brichkin, A. S.; Ivanov, S. V.; Toropov, A. A. *Phys. Rev. B* **2005**, *72*, 045302.

(8) Lee, S.; Dobrowolska, M.; Furdyna, J. K. *J. Appl. Phys.* **2006**, *99*, 08F702.

(9) Schmidt, T.; Scheibner, M.; Worschech, L.; Forchel, A.; Slobodskyy, T.; Molenkamp, L. W. *J. Appl. Phys.* **2006**, *100*, 123109.

(10) Erwin, S. C.; Zu, L. J.; Haftel, M. I.; Efros, A. L.; Kennedy, T. A.; Norris, D. J. *Nature* **2005**, *436*, 91–94.

(11) Archer, P. I.; Santangelo, S. A.; Gamelin, D. R. *Nano Lett.* **2007**, *7*, 1037–1043.

(12) Beaulac, R.; Archer, P. I.; Liu, X.; Lee, S.; Salley, G. M.; Dobrowolska, M.; Furdyna, J. K.; Gamelin, D. R. *Nano Lett.* **2008**, *8*, 1197–1201.

(13) Seufert, J.; Bacher, G.; Scheibner, M.; Forchel, A.; Lee, S.; Dobrowolska, M.; Furdyna, J. K. *Phys. Rev. Lett.* **2002**, *88*, 027402.

(14) Archer, P. I.; Santangelo, S. A.; Gamelin, D. R. *J. Am. Chem. Soc.* **2007**, *129*, 9808–9818.

(15) de Mello Donegá, C.; Bode, M.; Meijerink, A. *Phys. Rev. B* **2006**, *74*, 085320.

(16) de Mello Donegá, C.; Hickey, S. G.; Wuister, S. F.; Vanmaekelbergh, D.; Meijerink, A. *J. Phys. Chem B* **2003**, *107*, 489–496.

(17) Fisher, B. R.; Eisler, H.-J.; Stott, N. E.; Bawendi, M. G. *J. Phys. Chem. B* **2004**, *108*, 143–148.

(18) Crooker, S. A.; Barrick, T.; Hollingsworth, J. A.; Klimov, V. I. *Appl. Phys. Lett.* **2003**, *82*, 2793–2795.

(19) Lundstrom, T.; Schoenfeld, W.; Lee, H.; Petroff, P. M. *Science* **1999**, *286*, 2312–2314.

(20) Winbow, A. G.; Hammack, A. T.; Butov, L. V.; Gossard, A. C. *Nano Lett.* **2007**, *7*, 1349–1351.

(21) Kraus, R. M.; Lagoudakis, P. G.; Rogach, A. L.; Talapin, D. V.; Weller, H.; Lupton, J. M.; Feldmann, J. *Phys. Rev. Lett.* **2007**, *98*, 017401.